*Biochimica et Biophysica Acta*, 508 (1978) 27—38


BBA 77953

# FLUORESCENCE MEASUREMENTS OF ENVIRONMENTAL RELAXATION AT THE LIPID-WATER INTERFACE REGION OF BILAYER MEMBRANES *

J. HAMILTON EASTER, ROBERT P. DETOMA and LUDWIG BRAND

*Biology Department and McCollum-Pratt Institute, The Johns Hopkins University, Baltimore, Md. 21218 (U.S.A.)*

(Received August 15th, 1977)

## Summary

Nanosecond time-resolved emission spectroscopy is used to characterize the complex fluorescence behavior of the probe 2-*p*-toluidinonaphthalene 6-sulfonate (2,6 *p*-TNS) when adsorbed to several bilayer membrane system. These include egg phosphatidylcholine vesicles with and without added cholesterol as well as erythrocyte ghost membranes. In each case a nanosecond time-dependent shift of the fluorescence emission to lower energy follows pulsed photoexcitation. The properties of the time-resolved surfaces obtained are consistent with a non-exponential decay law which describes a continuous interaction process of 2,6 *p*-TNS with its local environment in the membrane. This environment consists in part of polar residues (water plus polar head region) undergoing nanosecond motions. The pure phosphatidylcholine bilayer system was studied at four temperatures and electronic and spectral relaxation contributions to the total fluorescence decay were separated. Temperature coefficients for empirical rate parameters derived for the separated processes were obtained. It appears that a treatment of the fluorescence behavior of amphiphilic probes such as 2,6 *p*-TNS adsorbed to bilayer membranes at temperatures near ambient in which a single lifetime and radiative decay channel have been assumed is inappropriate.

## Introduction

The molecule 2-*p*-toluidinonaphthalene 6-sulfonate (2,6 *p*-TNS) belongs to a class of fluorescence probes that has been widely used to obtain information

* Publication No. 933 from the McCollum-Pratt Institute.
Abbreviation: 2,6 *p*-TNS, 2-*p*-toluidinonaphthalene 6-sulfonate; ANS, anilinonaphthalene sulfonic acid.

regarding the polarity at specific sites on a variety of biomaterials [1]. The highly polar nature of the emitting excited states of 2,6 *p*-TNS and related molecules leads to fluorescence properties (spectral position and quantum yield) which depend greatly on the polarity of their environment. In a fluid polar solution the excited state solvation process is complete prior to fluorescence [2,3]. However, in a viscous medium like glycerol at room temperature solvation competes with fluorescence and the dynamics of solvent cage formation can be monitored on the nanosecond time scale by time-resolved emission spectroscopy [4]. Behavior corresponding to this later case has been observed with 2,6 *p*-TNS adsorbed to proteins [5—7] and to phosphatidylcholine vesicles [4,8]. In these protein and model membrane studies, the meaning of "solvent" may be extended to include residues of the macromolecule in the region of binding as well as solvent molecules in the neighborhood of this region which are likely to have different properties than those in the bulk solvent medium. The general term, environment, is appropriate for denoting this potentially anisotropic and heterogeneous "solvent" in such cases.

When environmental (solvent) relaxation and fluorescence emission occur on the same time scale, the fluorescence decay will be governed not only by electronic relaxation of the emitting population of excited molecules but also by the kinetics of the accompanying spectral shift (spectral relaxation). The fluorescence will be derived from a continuum or large number of discrete emitting levels and the resulting complex photokinetics will, in general, be non-exponential and emission wavelength dependent. A fluorescent system of this type cannot be considered as unitary [9] and a treatment in terms of a single fluorescence lifetime and a one-term quantum yield must be regarded in error.

In a previous report [4] we have shown that the fluorescence decay kinetics of 2,6 *p*-TNS absorbed to egg phosphatidylcholine vesicles can be described according to the Bakhshiev formulation of solvent relaxation. In this paper we study these kinetics in more detail by examining their temperature dependence and also extend this work to a real membrane system. The time-resolved fluorescence surface in each case has been separated into electronic and spectral relaxation components. In the vesicle system temperature coefficients have been determined for empirical decay parameters associated with each component process. In addition, the effect of added cholesterol at one temperature is examined. The nature of the interacting polar environment is discussed in terms of the assumed location of 2,6 *p*-TNS in the lipid bilayer.

## Experimental

*Materials.* Egg phosphatidylcholine was obtained from Sigma, St. Louis, Mo., and purified by absorption to activated silicic acid (UNISIL) as described by Hanahan [10]. The sample migrated as a single spot on thin-layer chromatography using two solvent systems (chloroform/methanol/water (65 : 25 : 4, v/v) and chloroform/methanol/acetic acid (7 : 3 : 1, v/v)) Iodine, ninhydrin and charring were used for detection.

Cholesterol was obtained from Applied Science Laboratories Inc. as 99% pure, lot No. 1828, and was used without further purification. Outdated whole blood was obtained from Union Memorial Hospital Blood Bank, Baltimore, Md.

The buffer used for the phosphatidylcholine and phosphatidylcholine-cholesterol vesicles was 0.1 M NaCl/0.1 M Tris · HCl in deionized water adjusted to pH 8.5. TRISMA Base was obtained from Sigma Chemical Co. The buffer used for the erythrocyte ghosts was isotonic phosphate-buffered saline, pH 7.39 (137 mM NaCl; 1.47 mM $KH_2PO_4$; 2.68 mM KCl; 8.10 $Na_2HPO_4$).

2,6 *p*-TNS were prepared by Seliskar and Brand [11], and all other chemicals were of laboratory reagent grade.

*Preparation of phosphatidylcholine and phosphatidylcholine-cholesterol vesicles.* The phosphatidylcholine vesicles were prepared by sonication under an argon atmosphere of approx. 100 mg of phosphatidylcholine in 3 ml of buffer (degassed with $N_2$ bubbling) for 1 h, followed by separation on Sepharose 4B (Pharmacia) as described by Huang [12]. For the phosphatidylcholine-cholesterol vesicles, 129 mg of phosphatidylcholine and 16 mg cholesterol (20 mol %) were co-dissolved in 2 ml of benzene and dried under reduced pressure at room temperature for 2 h. Sonication in 3.1 ml of degassed buffer and separation on Sepharose 4B was identical to that used with the phosphatidylcholine vesicles. The Sepharose 4B elution profile yielded two peaks (fraction I and II) and the vesicles (both phosphatidylcholine and phosphatidylcholine-cholesterol) were collected from the trailing side of the second peak where the fractions showed a linear relation between absorbance at 300 nm and lipid phosphorus.

*Preparation of erythrocyte ghosts.* Ghosts were prepared according to the procedure of Dodge et al. [13] using 22 mosm phosphate-buffered saline (pH 7.4) for lysis. The ghost pellet after the final wash had no pink color. The ghosts were readily visible under phase contrast microscopy and appeared round, re-sealed and their surface was smooth. The preparation was free from large or small debris. Ghost suspension with approx. five times the amount of 2,6 *p*-TNS used in the lifetime measurements and ghosts stained with pyrene were viewed under a fluorescence microscope. The ghosts (1) took up the dyes very uniformly, (2) showed little or no fluorescence debris, (3) appeared to "fill" with the dyes while still showing a very definite ring reaction, and (4) appeared to undergo no morphological changes upon addition of the dyes. The 2,6 *p*-TNS showed a noticeable amount of bleaching under the fluorescence microscope which, however, was not measureable in the steady state (Perkin-Elmer MRF-4) or lifetime fluorometer.

Though on a regular glass slide with a cover slip the ghosts were readily visible under phase contrast, it was not possible to count them on a hematocrit slide. The red blood cell count was $5.1 \cdot 10^9$ cells/ml, and since 25 ml of whole blood was used and the ghosts were taken up in 40 ml of phosphate-buffered saline, the ghost concentration would be $3.2 \cdot 10^9$ ghosts/ml with no losses during preparation. In addition, the cholesterol content of the ghost preparation was determined as 360 $\mu$g/ml. Dodge et al. [13] report an average value for cholesterol content of $1.29 \cdot 10^{-13}$ g/ghost; this would yield $2.8 \cdot 10^9$ ghosts/ml. Since some losses must occur during the preparation of the ghosts, the latter value would be expected to be lower and perhaps more reliable.

*Methods.* The determination of lipid phosphorus was by a modified procedure of Bartlett [14] and a colorimetric procedure for cholesterol determination was used [15]. Analysis of the phosphatidylcholine-cholesterol vesicles yielded 22 mol % cholesterol.

*Time-resolved emission spectra.* All decay curves were obtained on a monophoton fluorometer under single-photon conditions. The fluorometer was operated under fully automatic computer control, with semi-simultaneous collection of the decay curves and lamp profiles. Decay curves were collected from 2 to 10 nm intervals throughout the emission spectra. Excitation was with a 3300 Å narrow bandpass (8 nm) Baird-Atomic filter (No. 10-71-1). Emission was viewed through a monochromator with 2-mm slits (6.6 nm bandpass). The procedure for collection and analysis of the time-resolved emission data has been described previously [16]. All spectra are corrected for non-linear response of the detection system.

## Results

In agreement with the results of Huang and Charlton [17] a large fluorescence enhancement is observed when bilayer egg phosphatidylcholine vesicles are added to a solution of 2,6 *p*-TNS. The steady-state fluorescence spectra at −1°C and 32°C of 2,6 *p*-TNS adsorbed to vesicles are shown in Fig. 1. A small but significant red shift in the emission maximum with increasing temperature is observed, the origin of which will be explored by time-resolved fluorescence measurements.

Nanosecond time-resolved emission spectra were obtained with the 2,6 *p*-TNS · vesicle complex using a procedure described by Easter et al. [16]. Fluorescence decay curves were obtained at suitable wavelength intervals through the emission band. Impulse response functions were generated by an empirical deconvolution procedure making use of the method of non-linear least squares. These data required a minimum of three exponential terms to achieve satisfactory deconvolutions and the recovered decay parameters were emission wavelength dependent. In order to compare the decay characteristics at four temperatures the mean decay times are plotted as a function of emis-

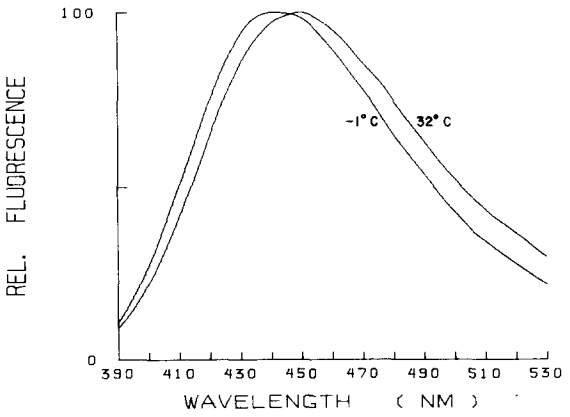


**Fig. 1. Steady-state fluorescence emission spectra of 2,6 *p*-TNS adsorbed to egg phosphatidylcholine vesicles at the temperatures indicated. Spectra are corrected for wavelength response and normalized. 2,6 *p*-TNS (12 μM), phosphatidylcholine (0.73 mM) at −1°C; 2,6 *p*-TNS (14.7 μM), phosphatidylcholine (0.81 mM) at 32°C.**

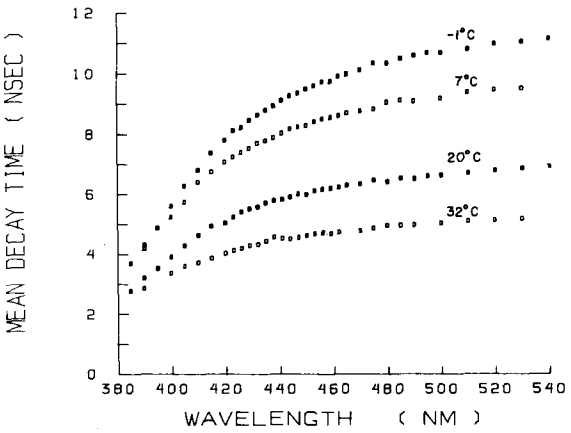


**Fig. 2. The mean decay time for 2,6 *p*-TNS adsorbed to phosphatidylcholine vesicles vs. wavelength is shown at the four temperatures indicated. Conditions are as described in the legend to Fig. 5. The mean fluorescence decay time is defined as**

$$\tau = \sum_{i=1}^{n} \alpha_i \tau_i^2 \Big/ \sum_{i=1}^{n} \alpha_i \tau_i$$

**where the alphas and taus are those obtained from the non-linear least squares empirical deconvolution.**

sion wavelength in Fig. 2. At a given temperature the mean decay time increases with wavelength and the overall magnitude of this change is observed to increase with decreasing temperature, the change being more pronounced at the red end of the emission. As will be shown later, this behavior is predictable in terms of the Bakhshiev formulation [18] of solvent relaxation.

2,6 *p*-TNS interacts with erythrocyte ghosts with an enhancement of fluorescence. The initial fluorescence enhancement occurs in less than 20 s and accounts for about 90% of the enhancement observed. A smaller fluorescence enhancement (about 10% of the total) foes to completion in about 3 min. This behavior is quite similar to that described by Freedman and Radda [19] for the interaction of 1,8-ANS with erythrocyte ghosts. A sample containing 20 $\mu$M 2,6 *p*-TNS and $10^8$ ghosts per ml was monitored for 8 h at 7°C and no change in fluorescence was observed after the initial 3 min increase.

The 2,6 *p*-TNS-erythrocyte ghost complex showed nanosecond time-dependent red shifts in the fluorescence emission spectra. Time-resolved spectra plotted as a function of emission energy at four representative times are shown in Fig. 3. In addition to the red shift with time these spectra retain a constant bandshape. This feature was also observed in every system reported here. The spectral relaxation kinetics describing the time dependence of the position of the emission maxima in energy units ($\nu_{max}$ vs. $t$) for the ghosts are shown in Fig. 4 along with the corresponding function for the pure vesicle system at 7°C.

Time-resolved emission spectra have also been obtained with 2,6 *p*-TNS adsorbed to egg phosphatidylcholine vesicles containing 22 mol % cholesterol. The spectral relaxation kinetics are also reported in Fig. 4 for the purpose of comparison. A very small increase in the rate of red shift is detected for the vesicle system when cholesterol is present. Clearly, more than the presence of

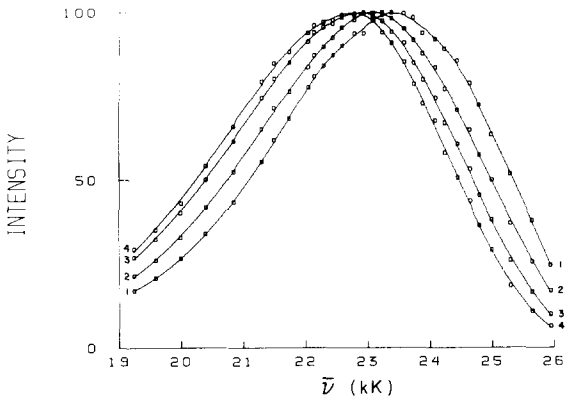


Fig. 3. Deconvolved nanosecond time-resolved emission spectra for 2,6 *p*-TNS (14 $\mu$M) adsorbed to erythrocyte ghosts ($10^8$ ghosts per ml) at 7°C. 1, 0.8 ns; 2, 4 ns; 3, 10 ns; 4, 16 ns after photo-excitation. These spectra have been peak normalized (kK = $10^3$ $cm^{-1}$).

cholesterol in the erythrocyte ghost system is required to define the different environments of 2,6 *p*-TNS in ghosts versus egg phosphatidylcholine vesicles as evidenced by their quite dissimilar spectral relaxation functions.

DeToma et al. [4] have shown that the Bakhshiev formulation of solvent relaxation [18] can be used to interpret the time-dependent red shifts observed with 2,6 *p*-TNS dissolved in glycerol or adsorbed to egg phosphatidylcholine vesicles. Accordingly, the fluorescence intensity at any time and energy, $I(\nu,t)$, is described as the product of an energy-independent electronic damping function, $i(t)$, and a dynamic spectral contour, $\rho(\nu - \nu_{max}(t))$, which shifts to low energy with time.

$$I(\bar{\nu}, t) = i(t)\rho(\bar{\nu} - \bar{\nu}_{max}(t)) \quad (1)$$

In the framework of this treatment $\rho(\nu,t)$ implicitly contains the spectral

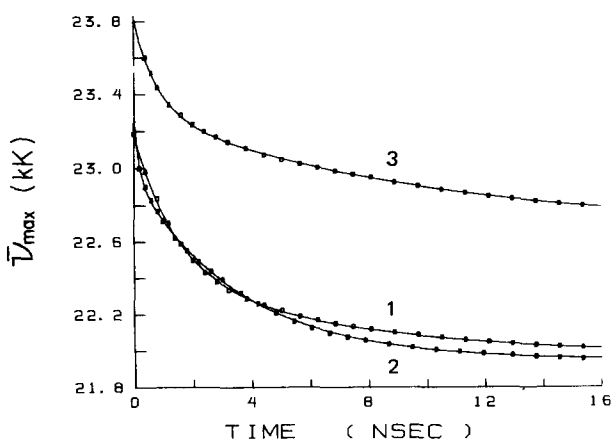


Fig. 4. The emission maxima ($\nu_{max}$) versus time for three systems all at 7°C. 1, 2,6 *p*-TNS (11 $\mu$M)-lecithin (0.86 mM); 2, 2,6 *p*-TNS (13.8 $\mu$M)-22 mol % cholesterol-phosphatidylcholine [cholesterol (0.20 mM): phosphatidylcholine (0.69 mM(]; and 3, 2,6 *p*-TNS (14 $\mu$M)-erythrocyte ghosts ($10^8$ per ml). An estimate from Dodge et al. [13] gives approx. 30 mol % cholesterol-lipid in ghosts.

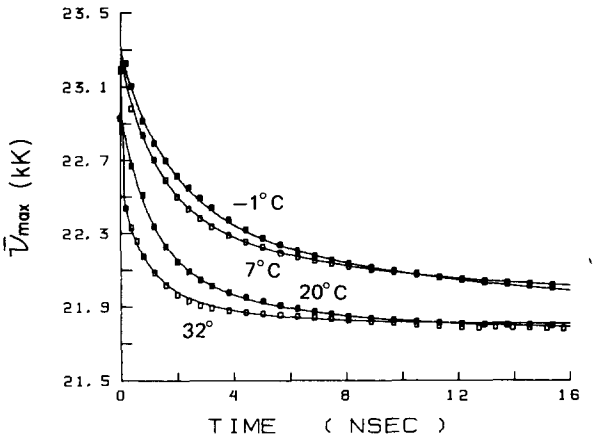


Fig. 5. The emission maxima ($\nu_{max}$) versus time are presented for 2,6 *p*-TNS adsorbed to egg phosphatidylcholine vesicles. Data points are connected by exponential analysis fits as described in text. 2,6 *p*-TNS (12 $\mu$M), phosphatidylcholine (0.73 mM) at −1°C; 2,6 *p*-TNS (11 $\mu$M), phosphatidylcholine (0.86 mM) at 7°C; 2,6 *p*-TNS (12.3 mM), phosphatidylcholine (0.84 mM) at 20°C; and 2,6 *p*-TNS (14.7 $\mu$M), phosphatidylcholine (0.81 mM) at 32°C.

relaxation function, $\nu_{max}(t)$, which is a direct measure of the environmental relaxation process that is taking place.

$\nu_{max}(t)$ representations were generated from time-resolved emission spectra for the system 2,6 *p*-TNS adsorbed to pure egg phosphatidylcholine vesicles at four temperatures (−1, 7, 20 and 32°C) and are illustrated in Fig. 5. These were analyzed empirically to a sum of exponentials that would best describe the data and a mean rate parameter ($k \equiv 1/\tau_\nu$) was calculated for each curve. An Arrhenius plot (In $k$ vs. $T^{-1}$) for these data was linear as shown in Fig. 6 and the positive temperature coefficient obtained from this plot is 6.43 kcal/mol.

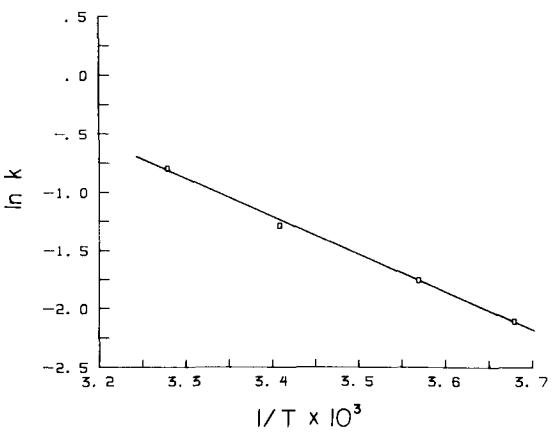


Fig. 6. An Arrhenius plot of the mean decay rates of $\nu_{max}(t)$ for 2,6 *p*-TNS adsorbed to egg phosphatidylcholine vesicles at the conditions described in the legend to Fig. 5. $T$ is the absolute temperature. $k$ is the mean decay rate, ($\tau_\nu^{-1}$), where

$$\tau_\nu = \sum_{i=1}^{n} \alpha_{\nu i}\, \tau_{\nu i}^2 \Big/ \sum_{i=1}^{n} \alpha_{\nu i}\, \tau_{\nu i}$$

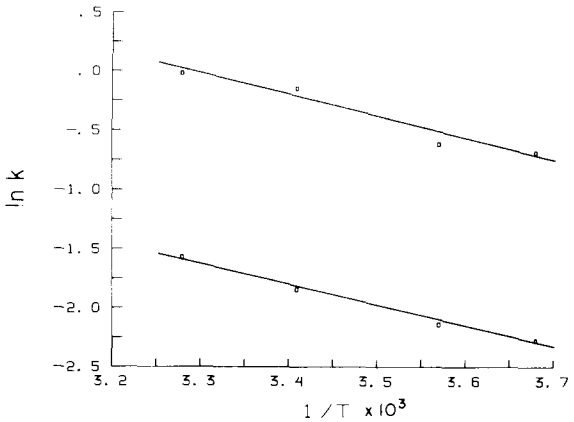


Fig. 7. An Arrhenius plot of the two rate parameters $\gamma_1$ and $\gamma_2$ obtained from the analysis of the electronic daming function $i(t)$, (see text, Eqn. 2) for 2,6 *p*-TNS adsorbed to egg phosphatidylcholine vesicles at the conditions described in the legend to Fig. 5. $T$ is the absolute temperature.

According to Eqn. 1 $\rho(\nu,t)$ contains the spectral influence of the environmental relaxation process on the observed fluorescence decay law, $I(\nu,t)$, and $i(t)$ describes the population decay kinetics characterizing the excited-state distribution of the fluorophore as the relaxation proceeds. The electronic damping function, $i(t)$ was obtained empirically from the time-resolved emission spectra following the procedure of DeToma et al. [4]. The function $i(i)$ was well described by a double exponential decay with parameters independent of emission wavelength for all three systems studied. The results of this analysis for the 2,6 *p*-TNS · erythrocyte ghost complex are remarkably similar to the phosphatidylcholine and glycerol systems shown by DeToma et al. [4].

The decay parameters for $i(t)$ obtained with the 2,6 *p*-TNS · vesicle complex at four temperatures are given in Table I. Arrhenius plots for $\gamma_1$ and $\gamma_2(ns^{-1})$ recovered for $i(t)$ show a linear dependence and are parallel as indicated in Fig. 7. An activation energy of 3.6 kcal/mol was obtained for both damping parameters $\gamma_1$ and $\gamma_2$. A double exponential analysis is also obtained for $i(t)$ with

TABLE I

EXPONENTIAL ANALYSIS OF THE DAMPING

Non-linear multiple regression analysis was used to fit the damping function to the model $i(t) = \beta_1 e^{-\gamma_1 t} + \beta_2 e^{-\gamma_2 t}$. The results presented here are the average of 28—34 analyses.

| System | Temperature (°C) | $\gamma_1^{-1}$ (ns) | $\gamma_2^{-1}$ (ns) | $\beta_1/\beta_2$ |
|---|---|---|---|---|
| Phosphatidylcholine | −1 | 1.98 | 9.73 | 0.396 |
| Phosphatidylcholine | 7 | 1.85 | 8.51 | 0.358 |
| Phosphatidylcholine | 20 | 1.16 | 6.33 | 0.427 |
| Phosphatidylcholine | 32 | 1.02 | 4.79 | 0.472 |
| Ghosts | 7 | 3.06 | 11.2 | 0.420 |
| 20 mol% cholesterol-phosphatidylcholine | 7 | 2.00 | 8.90 | 0.409 |

2,6 *p*-TNS bound to vesicles containing 22 mol % cholesterol yielding parameters $\gamma_1$ and $\gamma_2$ which are independent of emission wavenumber. The values are given in Table I which also includes the parameters for $i(t)$ obtained with 2,6 *p*-TNS · erythrocyte ghost complex.

## Discussion

Time-resolved emission spectroscopy can provide information regarding interactions between an excited chromophore and surrounding polar residues. These measurements can be used to characterize the environment and reflect events taking place on the nanosecond time scale.

An important feature of the data obtained with the vesicles as well as with the erythrocyte ghosts is that a nanosecond time-dependent red shift of the fluorescence emission spectrum is observed with all the systems described here. Such shifts are not observed with similar probes dissolved in non-polar solvents, since polar residues are required for the excited-state interaction. They are also not observed with these dyes dissolved in liquid non-viscous polar solvents. In these situations the excited-stated interactions do take place, but on a time-scale too rapid to be resolved by a nanosecond fluorometer. Time-dependent red shifts on the nanosecond time-scale are observed when 2,6 *p*-TNS is dissolved in viscous polar solvents such as glycerol. The experiments described here thus provide direct evidence that the probe bound to the vesicles or to the erythrocyte ghosts is surrounded by polar residues whose mobility is restricted as compared to liquid solutions.

The time-resolved spectral data obtained in this study describe a continuous interaction process of polar residues in the vicinity of the excited fluorophor according to Eqn. 1. This decay law is expressed as the product of two functions $i(t)$ and $\rho(\nu - \nu_{max}(t))$ which, respectively, define the electronic and spectral relaxation contributions to the total fluorescence decay. These functions are in turn characterized by the empirical parameters $\beta_j$, $\gamma_j$, $\nu_o$, $\nu_\infty$, $\alpha_{\nu j}$, $\tau_{\nu j}$, accordingly

$$i(t) = \beta_1 \, e^{-\gamma_1 t} + \beta_2 \, e^{-\gamma_2 t} \tag{2}$$

$$\nu_{max}(t) = \bar{\nu}_\infty + (\bar{\nu}_0 - \bar{\nu}_\infty) \sum_{j=1}^{n} \alpha_{\nu_j} \, e^{-t/\tau_{\nu j}} \tag{3}$$

The complex fluorescence decay kinetics for the 2,6 *p*-TNS · vesicle system and the corresponding mean decay times ($\tau$) shown in Fig. 2 that were derived from these data are readily explained by the decay law represented in Eqs. 1—3. The observed temperature dependence at a given wavelength reflects the changed relation between $i(t)$ and $\nu_{max}(t)$ induced with temperature. The strongest wavelength dependence is observed at the lower temperatures where the rates of decay of $i(t)$ and $\nu_{max}(t)$ are most comparable. We have observed that for structureless emission spectra Eqn. 1 predicts that the fluorescence decay in the region of the emission maxima is nearly monoexponential * with a

* Here $\rho(\nu, t)$ is almost flat except for a dip at early times which annihilates the $\beta_1 \, e^{-\gamma_1 t}$ contribution to Eqn. 2.

decay time approximately equal to $\gamma_2^{-1}$ of Eqn. 2. Hence, if fluorescence decay data governed by Eqn. 1 is only obtained in the region of the emission maximum it is easy to become mislead into believing that the total fluorescence response decays as a monoexponential.

In the framework of Eqn. 1 it is the function $i(t)$ which determines the steady-state fluorescence quantum yield of the system ($\phi_f = \int_0^\infty \int_0^\infty I(\nu,t)d\nu dt = \int_0^\infty i(t)dt$). $i(t)$ was recovered empirically as a sum of two exponentials for each system in this work. Since 2,6 *p*-TNS and related fluorescence probes exhibit a strong dependence of $\phi_f$ on solvent polarity, a likely interpretation for most of the non-monoexponential character of $i(t)$ is that the prevailing radiative and radiationless rate parameters depend on the relaxation state of the system and are, therefore, time dependent.

The results obtained with the single-bilayer egg phosphatidylcholine vesicles are best considered in relation to the probable location of 2,6 *p*-TNS. Stopped-flow kinetic measurements by Tsong [20] indicate that transport of the related probe 1,8-ANS across the bilayer of dimyristoyl phosphatidylcholine vesicles only occurs appreciably near the gel-to-liquid crystalline phase transition temperature. This finding suggests that when the dye is added to the vesicles above the transition temperature it attaches to the outer surface and does not penetrate significantly into the inner surface of the bilayer. Huang and Charlton [17] studied the binding of 2,6 *p*-TNS to bilayer vesicles and concluded that it binds with the toluidinyl group associated with the outer hydrocarbon region of the bilayer and the sulfonate anion near the polar choline head group. This is in agreement with Lesslauer et al. [21], Badley et al. [22] and Haynes and Staerk [23] who proposed that the probe 1,8-ANS binds with the phenyl group penetrating a short distance between the fatty acid chains of the hydrocarbon core.

The time-resolved emission maxima show an increase in the rate of the red shift of the emission spectra with time as the temperature is increased. This time-dependent lowering of the emission energy is attributed to the interaction of 2,6 *p*-TNS in its excited state with polar molecules in its vicinity. These molecules are most likely water although interaction with the polar choline and phosphate head groups of the lipid cannot be excluded.

The hydration of phospholipids has been thoroughly studied [24—28]. The water associated with the vesicles consists of a bulk water phase and a tightly bound phase. The bulk phase is weakly bound and resembles free water in that it is available to solvate solutes such as sucrose. The tightly bound phase is due to formation of a hydrate structure associated with the polar head groups. The amount of this bound water is dependent upon the nature of the polar head-groups [29]. Katz and Diamond [28] have indicated that the amount of bulk water and bound water increase with increasing temperature and that this may reflect an expansion in the area of the phosphatidylcholine bilayer with increasing temperature. The effect of temperature on the rate of the nanosecond time-dependent spectral shofts may reflect increasing mobility of the bound water phase with increasing temperature. It is of interest that the activation energy obtained from the $\nu_{max}(t)$ plot at the four temperatures is close to the 4—8 kcal/mol which can be associated with hydrogen bond energies. An alternative interpretation of the spectralshift data is that the "off" velocity of

the dye increases in the excited state and the shift of the spectra to lower energy at long times may reflect emission from dye molecules on their way out of the bilayer. Our measurements at present cannot distinguish among these possibilities.

The linear Arrhenius behavior for rate parameters derived from both the $i(t)$ and $\nu_{max}(t)$ representations is surprising in view of their potentially complex structure (involving many rate constants) and their empirical nature. Indeed, the narrow temperature range examined was probably not sufficient to separate lumped constants yet the analysis over this temperature range does provide an attractively simple description in that it emphasizes the smooth and continuous nature of the relaxation processes in this vesicle system. It would be interesting to obtain corresponding data over a larger temperature range or for a vesicle system which exhibits a sharp melting transition.

Newman and Huang [30] have presented evidence that egg phosphatidylcholine bilayer vesicles remain spherical and show no gross structural changes upon addition of up to 32 mol % cholesterol. The addition of cholesterol to the phosphatidylcholine vesicles can be expected to open up the polar head region due to the insertion of a hydrophobic group with no associated polar head group. While there is no direct evidence that cholesterol mixes randomly with phosphatidylcholine bilayers, Haynes and Staerk [23] report a statistical model which indicated that they do so. Ladbrooke et al. [31] inferred from X-ray diffraction work that there is an increase in the water layer upon addition of cholesterol to phosphatidylcholine bilayers. Newman and Huang [30] showed that the water-binding capacity of phosphatidylcholine-cholesterol vesicles increases with increasing cholesterol up to about 22 mol %.

The rate of the nanosecond time-dependent red shift for the 2,6 *p*-TNS · cholesterol-vesicle system shows a very slight increase as compared to the system without cholesterol at the same temperature. Thus cholesterol might alter the mobility of the bound water. Brockerhoff [32] emphasizes the capacity of cholesterol to donate a hydrogen bond, thus the 3$\beta$-OH group of the cholesterol could itself interact with the 2,6 *p*-TNS.

Erythrocyte ghosts represent a more complex system than bilayer vesicles. Freedman and Radda [19] showed that the binding of 1,8-ANS was complex and Weidekamm et al. [33] concluded that 1,8-ANS binds to membrane proteins. 2,6 *p*-TNS might be bound to proteins, to lipo-protein complexes, or in lipid domains.

The nanosecond time-resolved emission spectra observed with 2,6 *p*-TNS bound to erythrocyte ghosts indicate the presence of mobile polar residues in the environment of the probe. The values obtained for $\nu_0$ and $\nu_\infty$ suggest that the site may be more hydrophobic than is the case with phosphatidylcholine vesicles.

**Acknowledgements**

We thank Drs. Saul Roseman, Richard Pagano and Betty Gaffney for helpful discussions. We thank Dr. Joel Novros for assistance in the preparation of the erythrocyte ghosts. This work was supported by N.I.H. grant No. GM 11632. J.H.E. was supported by N.I.H. Training Grant No. GM-5T01-G57, R.P.D. by

N.I.H. Postdoctoral Fellowship No. 1F32GM01268 anf L.B. by N.I.H. Career Award Development Grant No. GM10245.

## References

1 Brand, L. and Gohlke, J.R. (1972) Annu. Rev. Biochem. 41, 843—868
2 Lippert, E. (1975) in Organic Molecular Photophysics (Birks, J.B., ed.), Vol. 2, pp. 1—31, Wiley, New York
3 DeToma, R.P. and Brand, L. (1977) Chem. Phys. Letts. 47, 231—236
4 DeToma, R.P., Easter, J.H. and Brand, L. (1976) J. Am. Chem. Soc. 98, 5001—5007
5 Brand, L. and Gohlke, J.R. (1971) J. Biol. Chem. 246, 2317—2319
6 Thorndill, D.T. (1973) Ph.D. dissertation. The Johns Hopkins University, Baltimore, Md.
7 Gafni, A., DeToma, R.P., Monroe, R.E. and Brand, L. (1977) Biophys. J. 17, 155—168
8 Easter, J.H. and Brand, L. (1973) Biochem. Biophys. Res. Commun. 52, 1086—1092
9 Birks, J.B. (1975) in Organic Molecular Photophysics (Birks, J.B., eds.), Vol. 2, p. 557, Wiley, New York
10 Hanahan, D.J. (1961) in Biochemical Preparations (Meister, A., ed.), Vol. 8, p. 121, Wiley, New York
11 Seliskar, C.J. and Brand, L. (1971) J. Am. Chem. Soc. 93, 5405—5414
12 Huang, C. (1969) Biochemistry 8, 344—352
13 Dodge, J.T., Mitchell, C. and Hanahan, D.J. (1963) Arch. Biochem. Biophys. 100, 119—130
14 Bartlett, G.R. (1959) J. Biol. Chem. 234, 466—468
15 Zlatkis, A., Zak, B. and Boyle, A.J. (1953) J. Lab. Clin. Med. 41, 486—492
16 Easter, J.H., DeToma, R.P. and Brand, L. (1976) Biophys. J. 16, 571—583
17 Huang, C. and Charlton, J.P. (1972) Biochemistry 11, 735—740
18 Bakhshiev, N.G., Mazurenko, Y.T. and Piterskaya, I.V. (1966) Opt. Spectrosc. 21, 307—309
19 Freedman, R.B. and Radda, G.K. (1969) FEBS Letts. 3, 150—152
20 Tsong, T.Y. (1975) Biochemistry 14, 5409—5414
21 Lesslauer, W., Cain, J.E. and Blasie, J.K. (1971) Biochim. Biophys. Acta 241, 547—566
22 Badley, R.A., Martin, W.G. and Schneider, H. (1973) Biochemistry 12, 268—275
23 Haynes, D.H. and Staerk, H. (1974) J. Membrane Biol. 17, 313—340
24 Small, D.M. (1967) J. Lipid Res. 8, 551—557
25 Chapman, D., Williams, R.M. and Ladbrooke, B.D. (1967) Chem. Phys. Lipids 1, 445—475
26 Huang, C. and Charlton, J.P. (1971) J. Biol. Chem. 246, 2555—2560
27 Finer, E.G. and Darke, A. (1974) Chem. Phys. Lipids 12, 1—16
28 Katz, Y. and Diamond, J.M. (1974) J. Membrane Biol. 17, 87—100
29 Chapman, D. (1975) Q. Rev. Biophys. 8, 185—235
30 Newman, G.C. and Huang, C. (1975) Biochemistry 14, 3363—3370
31 Ladbrooke, B.D., Williams, R.M. and Chapman, D. (1968) Biochim. Biophys. Acta 150, 333—340
32 Brockerhoff, H. (1974) Lipids 9, 645—650
33 Weidekamm, E., Wallach, D.F.H. and Fischer, H. (1971) Biochim. Biophys. Acta 241, 770—778